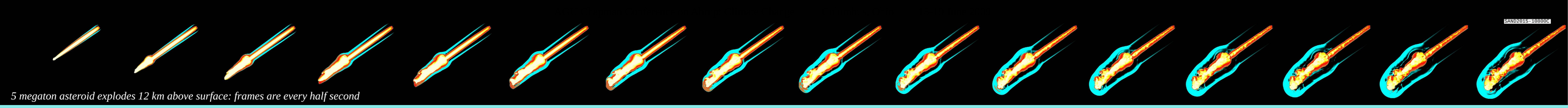

Can Plume-Forming Asteroid Airbursts Generate Meteotsunami in Deep Water?

Mark Boslough
Sandia National Laboratories
Albuquerque, NM 87185-0370
mbboslo@sandia.gov

Christopher Moore
NOAA Tsunami Research
NOAA Pacific Marine Environmental Lab
7600 Sand Point Way NE
Seattle, WA 98115
christopher.moore@noaa.gov

Vasily Titov
NOAA Tsunami Research
NOAA Pacific Marine Environmental Lab
7600 Sand Point Way NE
Seattle, WA 98115
vasily.titov@noaa.gov

Hydrocode simulations suggest that the 1908 Tunguska explosion was a plume-forming airburst analogous to those caused by Comet Shoemaker-Levy 9 (SL9) collisions with Jupiter in 1994. A noctilucent cloud that appeared over Europe following the Tunguska event is similar to post-impact features on Jupiter, consistent with a collapsed plume containing condensation from the vaporized asteroid and atmospheric water. Previous workers treated Tunguska as a point explosion and used seismic records, barograms, and extent of fallen trees to determine explosive yield. Estimates were based on scaling laws derived from nuclear weapons data, neglecting directionality, mass, and momentum of the asteroid. This point-source assumption, with other simplifications, led to a significant overestimate.

We suggest that coupling from an over-water plume-forming airburst could be a more efficient tsunami source mechanism than a collapsing impact cavity or direct air blast because the characteristic time of the plume is closer to that of a long-period wave in deep water. As the plume accelerates upward, it creates a slowly-rising and sustained overpressure that propagates outward at the speed of sound, generating a tsunami in deep ocean by the same mechanism that yields slower meteotsunami in shallow basins. This hypothesis is consistent with the Hubble Space Telescope (HST) observation of prominent internal waves observed propagating radially outward from several SL9 impacts, even though the waves were not in a Proudman resonance. The SL9 waves grew with a Froude number of ~1.6, the same as that of the sound speed in air over ~4.6-km-deep water on Earth.

Shoemaker-Levy 9: Plume-forming airbursts on Jupiter

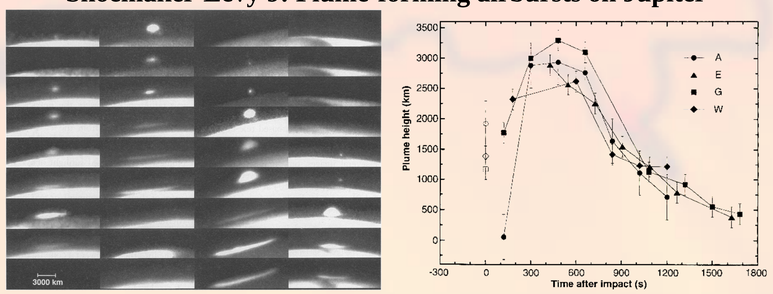

Left: Each column is a time sequence of Hubble Space Telescope (HST) images of plumes generated by four comet fragment impacts on Jupiter (A,E,G, & W respectively). Plumes are ejected along entry track and then fall back to form noctilucent clouds. Right: Height of each plume as a function of time after impact. Reaction forces from ballistic plume growth and collapse create two pulses of transient overpressure separated by plume free fall. Both figures from Hammel et al., (1995).

"Meteotsunami" on Jupiter

According to Hammel et al. (1995), "In images taken within 3 hours of the larger impacts, we detected transient 'rings' that are most likely caused by atmospheric waves. The most dramatic example was the multiple ring system created by the large G fragment. The circularity of the rings suggests that they are waves; debris features are asymmetric."

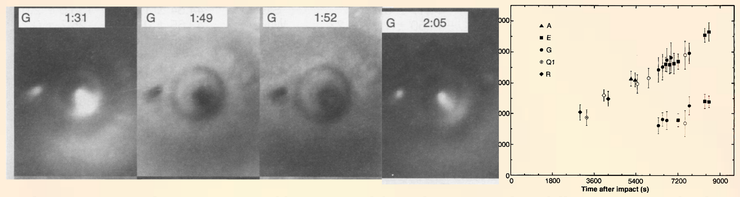

Left: HST images of waves generated by impact of the G fragment at four different times. Right: from Hammel et al. (1995), "Measurements of the positions of five main rings (upper cluster) and two secondary rings (lower cluster) are plotted as a function of elapsed time since impact… Open points are 889-nm methane-band images..."

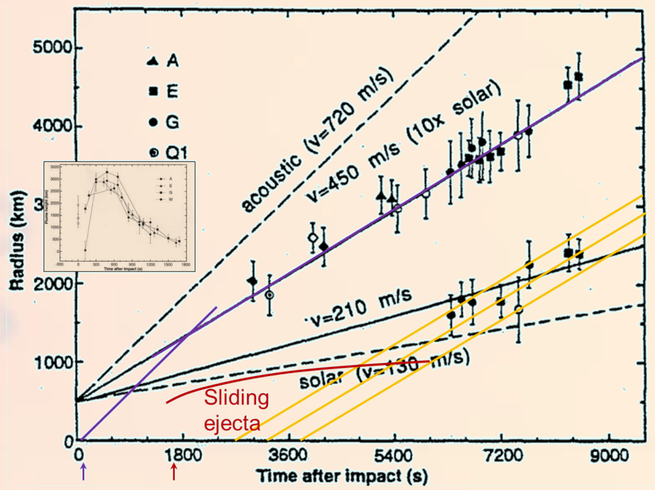

According to Hammel et al. (1995), "The best-fit line to the main ring observations does not cross through the origin, probably because of the sites' finite sizes at the time of wave creation. The slope of the line for the main ring is the wave propagation speed (454 ± 20 m s-1). The slope of the inner ring is not well constrained, but probably lies between 180 and 350 m s- 1. Because the wave speed appears to be constant for impacts of varying sizes (G produced a much larger disturbance than A, for example), we infer that the propagation velocity is independent of explosion energy, which implies a linear wave."

Ingersoll & Kanamori (1996) attribute these features to internal gravity waves: 'The intercept was determined from the fit to the upper set of points. "Acoustic" refers to the speed of sound at the temperature minimum. "Solar" and "10× solar" refer to the speed of a gravity wave in the water cloud with solar and 10× solar abundance of water.'

We suggest that these waves are the internal gravity wave equivalent of meteotsunami driven by the plume ejection and collapse. Overpressure associated with the explosion and plume ejection propagates radially (steep purple line) at the acoustic speed from the origin (purple arrow) and couples to the internal wave (shallow purple line) before the time of its first observation. The plume reenters and compresses the surface over a large area at a later time (red arrow). Ejecta slides radially (red curve) and drives a second internal wave (yellow) with the same speed as the first, but with different starting times for the three fragments for which it was observed.

Tunguska: Plume-forming airburst on Earth

Boslough and Crawford (1997) used the Sandia hydrocode CTH to model the energy deposition from a 15 megaton airburst on Earth, resulting in the growth and collapse of a plume containing tropospheric water and meteoritic vapor. Condensation is distributed over distances of thousands of kilometers at mesospheric altitudes, consistent with the bright night skies that are evidence of a noctilucent cloud similar to those observed by HST on Jupiter after collapse of SL9 plumes.

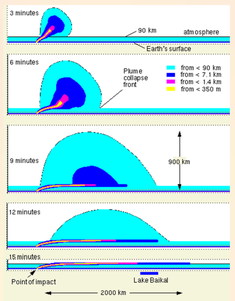

Left: Ballistic plume from a 15-megaton Tunguska-like airburst (Boslough & Crawford, 1997). Right: Distribution of bright night skies, June 30 – July 1, 1908 described by Zotkin (1961).

Sandia is a multiprogram laboratory operated by Sandia Corporation, a Lockheed Martin Company, for the United States Department of Energy under Contract DE-AC04-94AL85000.

Airburst-coupled meteotsunami: Preliminary modeling results

We ran a 2D cylindrical (vertical impact) plume-resolving simulation of a 5 megaton airburst at about 10 km above a reflecting surface. After the explosion, the jet of debris continues downward, pushing a bow shock ahead of it (the 3D version of this simulation is shown as sequence at top and bottom of poster). The associated overpressure is followed quickly by a suction phase and underpressure. The pressure change magnitude is about 0.1 atmosphere and takes place on timescales of several seconds. For the 2D case, surface pressure coupling is enhanced by plume ejection. The pressure disturbance at the surface propagates at the speed of sound, which is significantly faster than waves in all be the deepest ocean.

The mismatch in waves speed is represented by the Froude number (Fr = U/c) where U is the atmospheric disturbance translational speed and c= √gh is the longwave phase speed of ocean waves. Coupling is strongest at Proudman Resonance, when Fr ≈ 1.0. Ordinary meteotsunami are generated when strong weather fronts move across shallow water bodies with Fr ≈ 1.0. The much faster propagation associated with airbursts would only approach resonance in deep water. The ratio of acoustic to gravity wave speed observed on Jupiter yields Fr=1.6, the same as that for an airburst-driven tsunami in 4.6-km-deep water.

We generated a time-dependent boundary condition by converting pressure to wave height using the hydrostatic approximation as a crude preliminary model. This was intended to provide information about how the mismatch in wave speed will inhibit tsunami generation. The pressure wave propagates with a speed of about 348 m/s out to the edge of the domain (x = 50km).

We placed the impact 1000 km off of San Francisco, using Etopo1 for our tsunami model (MOST) bathymetry with dx=1 arcmin (1.85 km) resolution. Average water depths at impact are ~5000m, giving us a CFL time step of 3.2 sec, which we reduced to 2.0 sec to match hydrocode output files.

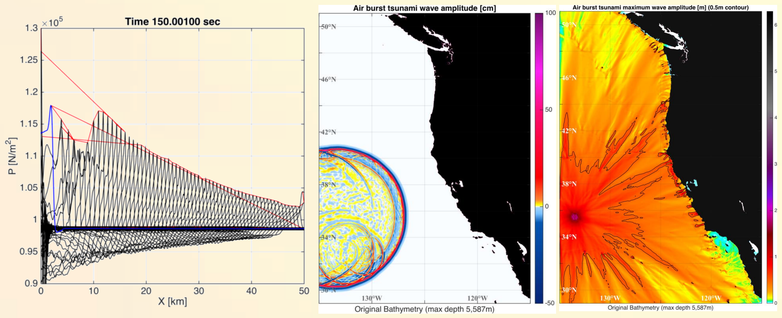

Left: Family of hydrocode-generated pressure profiles at surface for 5 megaton airburst at about 10 km altitude. Center: Single time step of tsunami generated by crudely coupling hydrocode output from airburst simulation to tsunami model. Right: Maximum wave amplitude of airburst-generated tsunami.

This simulation shows that the wave dissipates fast initially (as expected), but it still generates a very significant tsunami after the generation phase is passed, comparable with a very large earthquake-generated tsunami. A comparison run with deeper bathymetry (~11000m) shows much larger tsunami generation, consistent with Proudman resonance as the longwave speed is 331 m/s. This result needs to be confirmed with more simulations, refining runs, and sensitivity analysis.

Conclusions

Preliminary modeling suggests that Tunguska-scale plume-forming airburst can change atmospheric pressure over a large area on time scale sufficiently close to the Proudman resonance in deep water (~5 km) to produce dangerous meteotsunami. This effect needs to be further quantified and included in NEO hazard assessment.

References

Hammel, HB et al. (1995). HST Imaging of Atmospheric Phenomena Created by the Impact of Comet Shoemaker-Levy 9, *Science*, 267, 1288-1296.

Ingersoll, A. P., & Kanamori, H. (1996). Waves from the Shoemaker-Levy 9 impacts. *The Collision of Comet Shoemaker–Levy 9*, 329-345.

Boslough, MB & Crawford, DA (1997). Shoemaker-Levy 9 and plume-forming collisions on Earth. In *Near-Earth Objects*, J. Remo, editor, 236-282.

Zotkin, IT (1961). On anomalous optical effects in the atmosphere related to the Tunguska meteorite fall. *Meteoritica* 29:170-176.